Dalton Transactions

Accepted Manuscript

ROYAL SOCIETY OF CHEMISTRY

www.rsc.org/dalton

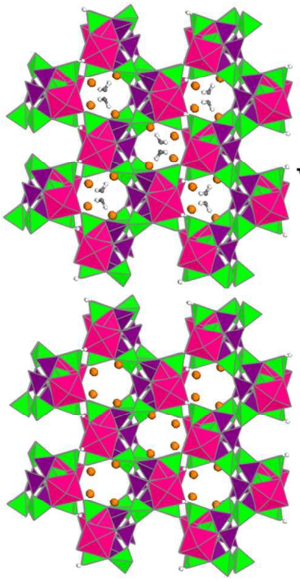

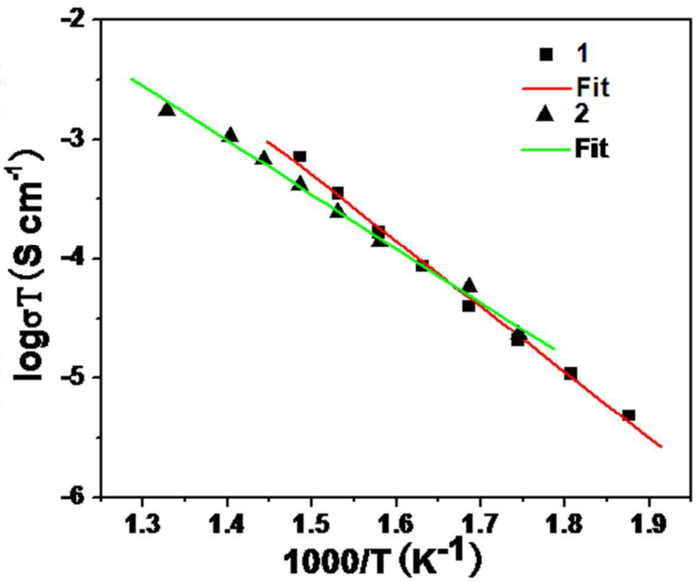

Two new isostructural metal borophosphates, $|K_2(H_2O)|[CoB_2P_3O_{12}(OH)]$ (**1**) and $|K_2(H_2O)|[NiB_2P_3O_{12}(OH)]$ (**2**), have been hydrothermally synthesized by ''green'' organotemplate-free route. Notably, the introduction of potassium ions in our synthetic system endows **1** and **2** with the K^+ ion conductivity rarely observed for borophosphates. What's more, the $|K_2(H_2O)|[MB_2P_3O_{12}(OH)]$ (M = Co, Ni) can remain the open framework after removal of guests-H_2O in the 8-MR channels by heating. The crystal structures of **1**, **1** heating 10h at 400 ^{o}C and plots of the bulk conductivity vs 1000/*T* are shown in TOC.

Journal Name

ARTICLE

Received 00th January 20xx,

Accepted 00th January 20xx

DOI: 10.1039/x0xx00000x

www.rsc.org/

Organotemplate-free synthesis of two open-framework metal borophosphates

Dan Zhang,[a] Yuquan Feng,[b] Yunling Liu,[a] Yuan Zhang,[a] Guanghua Li[a] and Hongming Yuan*[a]

Two new isostructural metal borophosphates, $|K_2(H_2O)|[CoB_2P_3O_{12}(OH)]$ [M = Co (**1**), Ni (**2**)], have been hydrothermally synthesized with non-polluting K^+ ions instead of organic template-ethylenediamine. Two metal borophosphates are isostructural and constructed by the connection of tetrahedral layers and MO_6 octahedra, giving rise to the 3-D intersecting 8-ring channels along the [010] direction. The negative charge of the framework is compensated by the K^+ ions located in the 8-ring channels. Like ethylenediamine, the K^+ ions also play an important structural directing role in the formation of the open framework. The framework shows a high thermal stability and is stable upon calcinations at ca. 400, 500 °C for **1** and **2**, respectively. Considering the motion of K^+ ions, ionic conductivities of two compounds were performed. The results indicated that they have similar activation energies of 0.94-1.09 eV and conductivities of 6.76×10^{-8}-9.88×10^{-8} S cm^{-1} at 320 °C.

Introduction

In recent years, metal borophosphates have attracted much attention because of their rich structural varieties and potential applications in magnetic, optical, ion-exchanging and electrochemical aspects.[1-7] Among these materials, organically-templated metal borophosphates are of great interest because of their potential for novel structures and, correspondingly, catalytic applications.[8] Since the first such borophosphate with an 3-D open framework structure, $|C_2H_{10}N_2|[CoB_2P_3O_{12}(OH)]$,[9] was reported ten years ago, a broad spectrum of organically-templated metal borophosphates with various dimensionalities and stoichiometries have been added to the list. Notable examples including $|C_4H_{16}N_3|[Zn_3B_3P_6O_{24}]\cdot H_2O$ with the CZP topology,[10] $|C_6H_{14}N_2|\{Zn[ZnB_2P_4O_{15}(OH)_2]\cdot(C_6H_{13}N_2)Cl\}$ featuring the first containing-Cl borophosphate,[11] $|(C_4H_{16}N_3)(C_4H_{15}N_3)_{0.5}|[Fe_2B_4P_7O_{26}(OH)_4]$[12] exhibiting interesting ferromagnetic behaviour below 9.6 K and $|(NH_4)_2(C_4H_{12}N_2)|[Co_2B_4P_6O_{24}(OH)_2]\cdot H_2O$[13] with a 3-D intersecting channel system have been reported. These compounds generally require organic amines or ammoniums as templates to direct the formation of a specific structure. However, the use of organic templates not only increases the synthetic cost, but also causes environmental pollution due to the release of reaction wastes. Moreover, the high temperature calcinations for the removal of organic templates result in high energy consumption, as well as structure collapse of some frameworks, thus greatly limiting their practical utility. It is highly desirable to develop a simple, low cost and ‘‘green’’ organotemplate-free route for the synthesis of those specific structure, and to further explore their practical applications. Recently, *Yu* et al. have successfully synthesized a few of aluminophosphates by using organotemplate-free route under hydrothermal conditions.[14-16] In this work, we have developed an organotemplate-free route for the synthesis of borophosphtes in the B_2O_3-P_2O_5-MO-K_2O-H_2O system, and successfully synthesized $|K_2(H_2O)|[CoB_2P_3O_{12}(OH)]$ (**1**) and $|K_2(H_2O)|[NiB_2P_3O_{12}(OH)]$ (**2**) with the same 3-D open framework under hydrothermal conditions. The 3-D open framework was first reported as $|C_2H_{10}N_2|[CoB_2P_3O_{12}(OH)]$ synthesized by using ethylenediamine as the template.[9] Its structure displays intersecting 3-D intersecting 8-ring channels. Several structurally related borophosphtes were also reported.[17-21] The organic templates, such as EDA, 1,2-DAP, 1,3-DAP, or PIP, were needed in these syntheses. Notably, the introduction of potassium ions in our synthetic system endows **1** and **2** with the small K^+ ion conductivity rarely observed for borophosphates. This work opens the possibility for the organotemplate-free synthesis of borophosphates, being simple, cost-effective and environmentally friendly.

Experimental

Synthesis

The two compounds were prepared under similar mild hydrothermal conditions. A mixture of H_3BO_3 (4.637 g, 75 mmol), $MCl_2\cdot 6H_2O$ (M = Co, Ni) (1.189 g, 5 mmol), KH_2PO_4 (4.763 g, 35 mmol) and 3 mL H_2O were directly added into a 15 mL Teflon-lined

---

[a] State Key Laboratory of Inorganic Synthesis and Preparative Chemistry, College of Chemistry, Jilin University, Changchun 130012, P.R. China. E-mail: hmyuan@jlu.edu.cn; Fax: +86-0431-85168318
[b] College of Chemistry and Pharmacy Engineering, Nanyang Normal University, Nanyang 473061, P.R. China

Electronic Supplementary Information (ESI) available. CCDC 1410100 (1) and 1410101 (2). For ESI and crystallographic data in CIF or other electronic format see DOI: 10.1039/x0xx00000x stainless steel autoclave and heated at 240 °C for 5 d. The final product, as rod-like single crystals, was washed with distilled water until the residual H_3BO_3 was completely removed and then dried in air.

Structure determination

Two suitable single crystals with dimensions 0.28 × 0.26 × 0.24 and 0.24 × 0.22 × 0.20 mm were selected for single-crystal X-ray diffraction analyses. The data were collected on a Bruker SMART CCD APEX II diffractometer using graphite-monochromated Mo-*Ka* radiation (λ = 0.71073 Å) at a temperature of 20±2 °C. Data processing was accomplished with the SAINT processing program .[22] Their structures were solved by direct method and refined by full matrix least-squares technique with the SHELXTL crystallographic software package.[23] The K, Co, B, P and O atoms of the framework could be unambiguously located. The H atoms associated with the hydroxy of the PO_4 group were added geometrically. Experimental details for the crystal determinations of **1** and **1** heating 10 h at 400 °C (**1-a**) are listed in Table 1. One K site in **1-a** exists thermal vibration, which does not affect the structure analysis.

Table 1. Crystal data and structure refinement for **1**, **1-a**.

	1	**1-a**
Empirical formula	$B_2CoH_3K_2O_{14}P_3$	$B_2CoHK_2O_{13}P_3$
Formula weight	478.68	460.67
Temperature/K	293(2)	293(2)
Wavelength/Å	0.71073	0.71073
Crystal system	Orthorhombic	Orthorhombic
Space group	*P b c a*	*P b c a*
a/Å	9.7255(7)	9.5543(19)
b/Å	12.2075(8)	12.056(2)
c/Å	19.9276(18)	19.814(4)
Volume/$Å^3$	2365.9(3)	2282.3(8)
Z	8	8
Density(calc.)/ Mg/m^3	2.688	2.681
Absorption coeff./mm^{-1}	2.641	2.726
F(000)	1880	1800
Crystal size/mm	0.28 × 0.26 × 0.24	0.24 × 0.22 × 0.20
Theta range/°	2.04 to 25.02	3.380 to 27.428
Limiting indices	-10<= *h* <=11 -14<= *k* <=14 -23<= *l* <=20	-11<= *h* <=12 -15<= *k* <=14 -25<= *k* <=25
Reflections collected/unique	12441 / 2092	20555 / 2591
R(int)	0.0561	0.0603
Data/restraints/ parameters	2092/4/205	2591/1/204
GOF on F^2	1.006	1.031
R indices [*I*>2*ó*(*I*)]	R_1 = 0.0265 wR_2 = 0.0716	R_1 = 0.0316 wR_2 = 0.0712
R indices (all data)	R_1 = 0.0317 wR_2 = 0.0760	R_1 = 0.0447 wR_2 = 0.0760
Largest diff. peak and hole/e.$Å^{-3}$	0.869 and -0.723	0.526 and -0.473

Measurements

X-Ray powder diffraction (XRD) data were collected on a Rigaku D-Max 2550 diffractometer with Cu-*Ka* radiation (λ = 1.5418 Å). Inductively coupled plasma (ICP) analyses were performed on a Perkin-Elmer Optima 3300Dv spectrometer. Thermogravimetric analysis (TGA) was carried out on a Perkin-Elmer TG-7 analyzer in air with a heating rate of 10 °C min^{-1}. The infrared (IR) spectrum was recorded within the 400-4000 cm^{-1} region on a Bruker-IFS 66V/S spectrometer using KBr pellets**.**

Ionic Conductivities

Impedance measurements were performed by using a Solartron SI 1287 electrochemical interface and a Solartron SI 1260 impedance/gain-phase analyzer. Pellets with ca.1.0-cm diameter and 1.0-mm thickness were prepared by cold pressing of the powder samples and were further sintered at 400 °C for 10 h to minimize the grain boundary effect. For a better contact, both sides of these pellets were coated with Ag powders and heated at 100 °C for 2 h. The scanning frequency ranged from 10^6 to 100 Hz, and the ac voltage applied was adjusted according to the resistance of each compound. The heating rate was kept at 3 °C min^{-1} from room temperature to 400 and 500 °C, respectively. The resistance of each compound was obtained from a circle fit of the impedance spectrum, and their conductivities were calculated by taking into account the thickness and area of the pellets.

Results and discussion

Synthesis and Characterization

$|K_2(H_2O)|[MB_2P_3O_{12}(OH)]$ (M = Co, Ni) could be prepared in the reaction mixtures with a optimal molar composition of 75 H_3BO_3 : 5 $MCl_2·4H_2O$ (M = Co, Ni) : 35KH_2PO_4 : 3 mL H_2O at 240 °C for 5 d, giving 50%, 20% yields based on Co and Ni, respectively. When the reaction temperature for Co was lower than 220 °C, the main product was $KCo(H_2O)_2BP_2O_8·0.48H_2O$.[24] Whereas, the crystal can't be obtained when the reaction temperature for Ni was lower than 240 °C. When H_3PO_4, LiH_2PO_4, NaH_2PO_4 and $NH_4H_2PO_4$ were used instead of KH_2PO_4, then isotypic compounds could not be obtained. It indicates that K^+ ions play an important structure directing role in the formation of the open framework of $|K_2(H_2O)|[MB_2P_3O_{12}(OH)]$ (M = Co, Ni). But, the crystal size of **2** is too small for single-crystal X-ray diffraction analysis. The two compounds could also be synthesized by using $M(OAc)_2·4H_2O$ (M = Co, Ni) under similar conditions. Anal. Calcd. (wt %) for **1**: K 16.34, Co 12.31, B 4.52, P 19.41; found: K 16.03, Co 12.36, B 4.60, P 19.46. Anal. Calcd. (wt %) for **2**: K 16.34, Ni 12.27, B 4.52, P 19.42; found: K 16.15, Ni 12.04, B 4.50, P 19.26.

The powder XRD pattern of as-prepared **1** and **2** (shown in Figure 1) are in agreement with the simulated one generated on the basis of the single-crystal structural data, suggesting that compound **1** and **2** are pure phase and isostructural to each other. Figure. S1 (Supporting Information) shows the result of Rietveld refinement for the powder XRD pattern of **2** using the crystal structure model presented by the single crystal XRD for **1**. The thermal properties of

$|K_2(H_2O)|[MB_2P_3O_{12}(OH)]$ (M = Co, Ni) were studied by TGA, and their TGA curves are shown in Figure S2 of the Supporting Information. The TGA experiments for compound **1** showed two steps of weight loss from about 25 to 800 ^{o}C. The weight loss within 25-400 ^{o}C is 4.1%, which corresponds to the release of the H_2O molecule (calcd 3.8%). The weight loss at the second step, 400-800 ^{o}C, is 2.0%, and this agrees with the removal of 0.5 molar equiv of water through condensation of P-OH groups (calcd 1.9%). The TGA results of compound **2** are similar to those of compound **1**, and their total weight losses are 6.3% (calcd: 5.7%). The TGA results of samples after heating 10 h at 400 ^{o}C only showed a step of weight loss(2.2% for **1**, 2.0% for **2**), which also agree with the removal of 0.5 molar equiv of water through condensation of P-OH groups, as shown in Figure S3 (Supporting Information). These results reveal that both **1** and **2** can remove the H_2O molecules and remain the P-OH group at 400 ^{o}C. XRD studies at different temperatures (Figure S4 of the Supporting Information) show that **1** and **2** have a high thermal stability and they can keep their structures intact upon calcinations at 400 and 500 ^{o}C, respectively. The powder XRD patterns of samples after heating migrate to the right direction slightly. This is probably due to the fact that the volume of the unit cell reduces with the removal of H_2O. The IR spectra of **1**, **1** heating 10 h at 400 ^{o}C (**1-a**), **2** and **2** heating 10 h at 400 ^{o}C are shown in Figure S5 and S6. The bands at 3607, 3421, 1652 cm^{-1} can be assigned to the stretching and bending vibrations of H_2O molecules, while these bands disappear after heating. It reveals that both **1** and **2** remove the H_2O molecules after heating, which is in agreement with the TGA analyses. The bands from 1250 to 400 cm^{-1} can be assigned to the asymmetric stretching and bending vibrations of PO_4, BO_4, and B-O-P groups.[25]

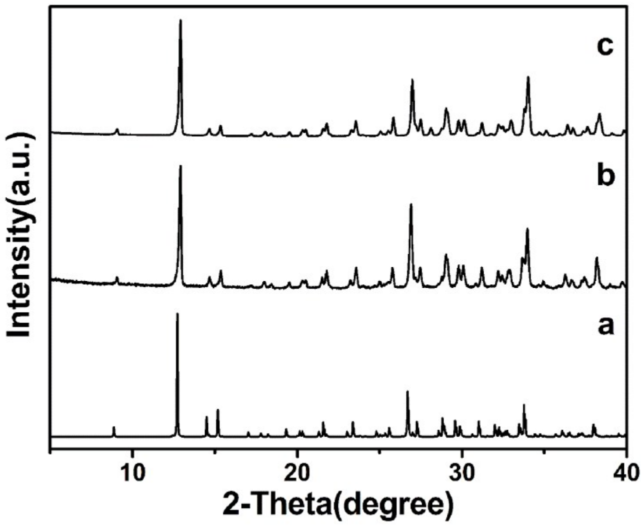

Figure 1. Simulated XRD (a), experimental XRD patterns of **1** (b) and **2** (c).

Structure description

The compounds $|K_2(H_2O)|[MB_2P_3O_{12}(OH)]$ (M = Co, Ni) are isostructural to each other, and crystallize in the space group *Pbca*. Here, we describe the structure of compound **1** as being representative. The single-crystal structural analysis reveals that the asymmetric unit of **1** contains one crystallographically unique Co atom, two crystallographically unique B atoms and three crystallographically unique P atoms (Figure 2). The Co atom is octahedrally coordinated by six oxygen atoms with the Co-O bond lengths ranging from 2.025(2) to 2.158(2) Å, where five oxygen atoms are shared by nearby P atoms and the other one oxygen is connected with nearby B atom, similar to those in known cobalt borophosphates.[26-28] All the B atoms are in a tetrahedral coordination, sharing three O atoms with neighbouring P atoms, leaving one O atom shared with Co atom (B-O bond lengths: 1.436(4) to 1.510(4) Å). All the P atoms are tetrahedrally coordinated to oxygen atoms, then further connected to adjacent Co and B atoms, while P(3) possess one terminal -OH group (P-O bond lengths: 1.497(2) to 1.588(2) Å). The B-O bond lengths and the P-O bond lengths fall in the typical bond length ranges.[29-32] The protons H11, H14A and H14B are attached to O11 and O14 , respectively [*d*(O11-H11) = 0.816(12) Å, *d*(O14-H14A) = 0.818(12) Å, *d*(O14-H14B) = 0.81 Å], and are involved in hydrogen bridges [O11-H11···O(2)#7 with *d*(O11···O(2)#7) = 2.685(3) Å, O14-H14A···O(13)#5 with *d*(O14···O(13)#5) = 2.816(4) Å, O14-H14B···O(3)#5 with *d*(O14···O(3)#5) = 3.046(4) Å and O14-H14B···O(10)#5 with *d*(O14···O(10)#5) = 3.135(4) Å. The selected bond lengths and angles of **1** and **1-a** are listed in Table S1 and S2.

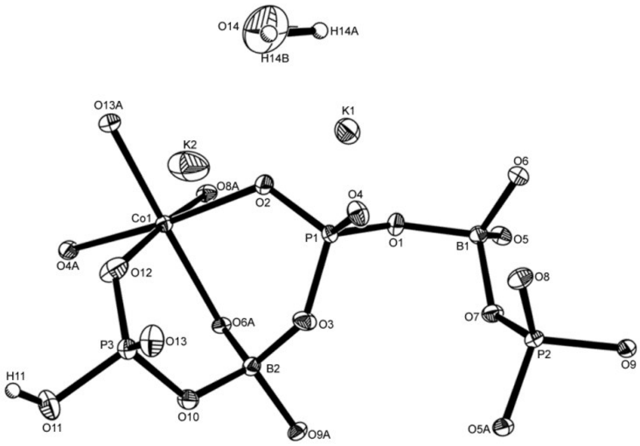

Figure 2. The thermal ellipsoid plots (50% probability) and atomic labelling schemes of 1.

Single-crystal structural analyses reveal that compound **1** possesses isostructural 3-D open framework crystallizing in the *Pbca* (No. 61) space group. They are closely related to the borophosphates with general formula $|C_2H_{10}N_2|[MB_2P_3O_{12}(OH)]$, where M = Mg, Mn, Fe, Co, Ni, Cu, Zn and Cd.[9,17,19] The overall crystal structure of **1** is characterized by stacking of the tetrahedral layers made of BO_4, PO_4 and $PO_3(OH)$ tetrahedra along [100] with the sequence *ABAB*... The CoO_6 octahedras act as fasteners between the layers to form a three-dimensional framework, as shown in Figure 3. The framework displays a system of intersecting 8-MR channels along [010] direction (Figure 4a). They are occupied by the K^+ ions and H_2O molecules that are stacked along [010] direction. The K^+ ions were coordinated with oxygen atoms belonging to the framework and H_2O molecules, which were fixed via O-H···O hydrogen bonds to the framework. The compound **1** after heating 10 h at 400 ^{o}C (**1-a**) also crystallizes in the *Pbca* (No. 61) space group. No H_2O molecules were assigned in the single-crystal structure of compound **1-a** (Figure 4b), although it is possible that a small amount of diffuse H_2O still occupies the voids of 8-MR channels. This is supported by the result of IR and thermal analyses. Comparing compound **1** with **1-a** reveals a rearrangement in molecular packing, but no significant change to the framework or the intersecting 8-MR channels along [010] direction. However, the volume of the unit cell was reduced *ca.* 83.6 Å^3 after the transformation of **1**, which is in accordance with the migration of XRD analysis. Compared to the $|C_2H_{10}N_2|[MB_2P_3O_{12}(OH)]$ with ethylenediamine as an organic template, the $|K_2(H_2O)|[MB_2P_3O_{12}(OH)]$ with K^+ ions has extreme advantages. First of all, K^+ ions are non-polluting and less expensive. Secondly, the $|K_2(H_2O)|[MB_2P_3O_{12}(OH)]$ can remain the open framework after removal of guests-H_2O in the 8-MR channels by heating. Whereas, the framework structure of $|C_2H_{10}N_2|[MB_2P_3O_{12}(OH)]$ collapse after removal of guests-ethylenediamine by heating.[18]

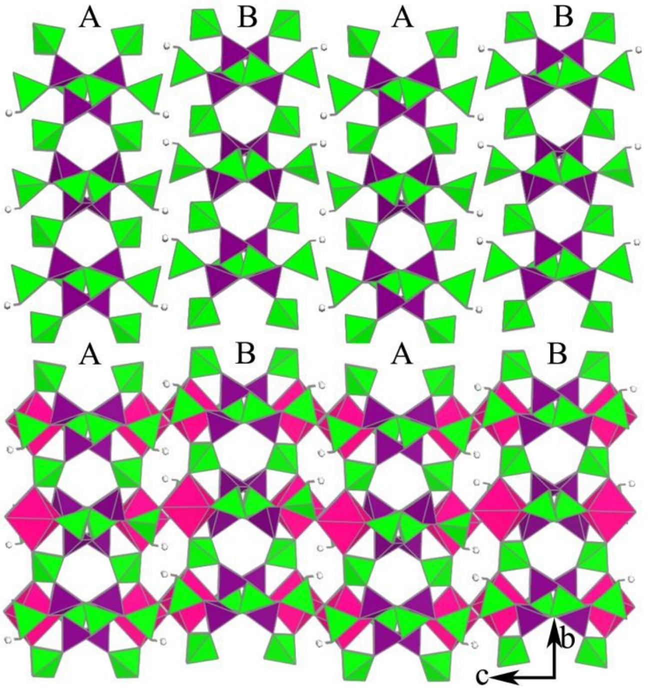

Figure 3. The tetrahedral layers of **1** along the [100] direction.

Ionic conductivities

The impedance measurements of $|K_2(H_2O)|[MB_2P_3O_{12}(OH)]$ (M = Co, Ni) were performed on sintered pellets. The plots of the bulk conductivity [log(ó*T*)] *vs* reciprocal temperature (1000/*T*) for these three compounds are shown in Figure 5. The data are well-fitted to the Arrhenius Expressions [ó = ó$_0$ exp(-*E*/*kT*), where ó$_0$ is a preexponential factor, *E* is the activation energy, and *k* is the Boltzmann constant]. The *E* and ó$_0$ parameters, together with the conductivities at 320 °C, are outlined in Table 2. Their *E* values fall in the range of 0.94-1.09 eV, and conductivities (ó) at 320 °C change from 6.76×10^{-8} to 9.88×10^{-8} S cm^{-1}. These data are comparable to those of reported $Na_4Ni_5(PO_4)_2(P_2O_7)_2$,[33] $Na_4M_3(PO_4)_2(P_2O_7)$ (M = Mn, Co, Ni),[34] $Na_5(H_3O)\{M_3[B_3O_3(OH)]_3(PO_4)_6\}\cdot 2H_2O$ (M = Mn, Co, Ni).[26] Compared with the good Na^+ ion conductors, such as NASICON, related NASICON compounds, and *β*-alumina,[35-39] however, the lower conductivity and higher activation energy of $|K_2(H_2O)|[MB_2P_3O_{12}(OH)]$ indicate that K^+ ions in these compounds move with difficulty.

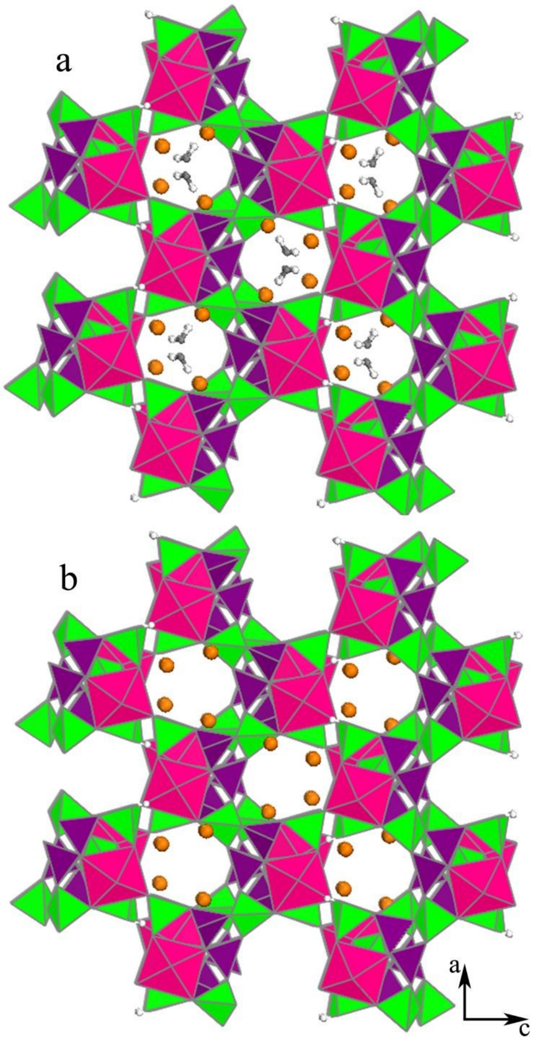

Figure 4. The crystal structures of **1** (a) and **1-a**(b).

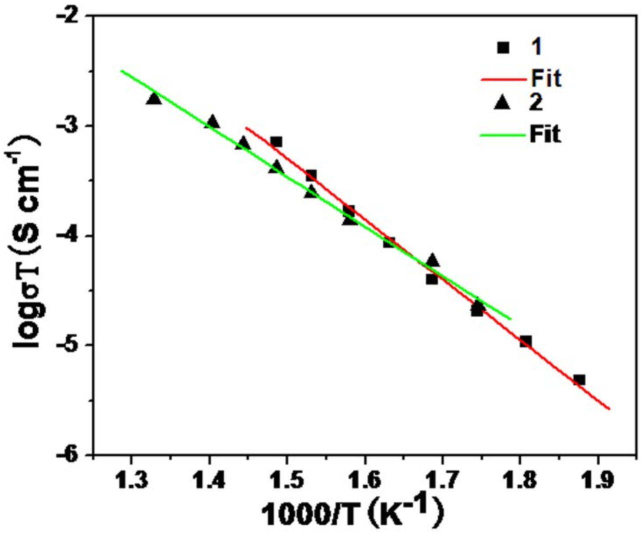

Figure 5. Plots of the bulk conductivity *vs* 1000/T for **1** and **2**. The straight lines are the best fits to the equation $ó = ó_0 \exp(-E/kT)$.

Table 2. Activation energies (E), preexponential factors ($ó_0$), and ionic conductivities at 320 °C ($ó_{320}$) for **1** and **2**.

Compound	E (eV)	$ó_0$ (S cm^{-1})	$ó_{320}$ (S cm^{-1})
1	1.09	119	6.76×10^{-8}
2	0.94	176	9.88×10^{-8}

Conclusions

Two new isostructural transition metal borophosphate, $|K_2(H_2O)|[MB_2P_3O_{12}(OH)]$ (M = Co, Ni), were successfully prepared by K^+ ions instead of organic template-ethylenediamine. Two compounds feature a 3-D system of intersecting 8-MR channels along [010] direction, which are occupied by the K^+ ions and H_2O molecules, just like $[C_2H_{10}N_2]^{2+}$ in $|C_2H_{10}N_2|[MB_2P_3O_{12}(OH)]$. The lower conductivity and higher activation energy of $|K_2(H_2O)|[MB_2P_3O_{12}(OH)]$ indicate that K^+ ions in these compounds move with difficulty. The successful synthesis of **1** and **2** reveals that the K^+ ions play an important structure directing role in the formation of these open frameworks. Compared to the $|C_2H_{10}N_2|[MB_2P_3O_{12}(OH)]$ with ethylenediamine as an organic template, the $|K_2(H_2O)|[MB_2P_3O_{12}(OH)]$ (M = Co, Ni) with K^+ ions have extreme advantage. This work will open new perspectives for the organotemplate-free synthesis of novel borophosphate materials with interesting properties and applications.

References

1 A. Yilmaz, X.-H. Bu, M. Kizilyalli and G. D. Stucky, *Chem. Mater.*, 2000, **12**, 3243.
2 B. Ewald, Y.-X. Huang and R. Kniep, *Z. Anorg. Allg. Chem.*, 2007, **633**, 1517.
3 W.-T. Yang, J.-Y. Li, Q.-H. Pan, Z. Jin, J.-H. Yu and R.-R. Xu, *Chem. Mater.*, 2008, **20**, 4900.
4 W.-T. Yang, J.-Y. Li, Q.-H. Pan, H.-Z. Xing, Y. Chen, J.-H. Yu and R.-R. Xu, *J. Mater. Chem.*, 2009, **19**, 4523.
5 M. Yang, J.-H. Yu, L. Shi, P. Chen, G.-H. Li, Y. Chen and, R.-R. Xu, *Chem. Mater.*, 2006, **18**, 476.
6 T. Yang, G.-B. Li, J. Ju, F.-H. Liao, M. Xiong and J.-H. Lin, *J. Solid State Chem.*, 2006, **179**, 2534.
7 L. Tao, G. Rousse, M. Sougrati, J. Chotard and C. Masquelier, *J. Phys. Chem. C*, 2015, **119**, 4540.
8 K. C. Anthony, F. Gerard and L. Thierry, *Angew. Chem. Int. Ed.,* 1999, **38**, 3268.
9 S. C. Sevov, *Angew. Chem.*, 1996, **108**, 2814.
10 W. Liu, M.-R. Li, H.-H. Chen, X.-X. Yang and J.-T. Zhao, *Dalton Trans.*, 2004, **18**, 2847.
11 Y. X. Huang, G. Schafer, W. Carrillo-Cabrera, H. Borrmann, R. C. Gil and R. Kniep, *Chem. Mater.*, 2003, **15**, 4930.
12 W.-T. Yang, J.-Y. Li, Q.-H. Pan, H.-Z. Xing, Y. Chen, J.-H. Yu and R.-R. Xu, *J. Mater. Chem.*, 2009, **19**, 4523.
13 W. Liu, X.-Q. Guo, G. Su, L.-X. Cao, Y.-G. Wang and J.-R. Duan, *J. Solid State Chem.*, 2011, **184**, 2538.
14 Y.-Y. Wang, Y. Mu, C.-Q. Zhang, J.-Y Li and J.-H Yu, *Chem. Commun.,* 2014, **50**, 15400.
15 Y. Mu, Y.-Y. Wang, Y. Li, J.-Y Li and J.-H Yu, *Chem. Commun.,* 2015, **51**, 2149.
16 Y.-J. Sun, Y. Y, Y.-Y. Wang, Y. Li, J.-Y Li and J.-H Yu, *Chem. Commun.,* 2015, **51**, 9317.
17 R. Kniep and G. Schafer, *Z. Anorg. Allg. Chem.*, 2000, **626**, 141.
18 G. Schafer, H. Borrmann and R. Kniep, *Z. Anorg. Allg. Chem.*, 2001, **627**, 61.
19 W. Liu, M.-H. Ge, X.-X. Yang, H.-H. Chen, M.-R. Li and J.-T. Zhao, *Inorg. Chem.*, 2004, **43**, 3910.
20 Y.X. Huang, O. Hochrein, D. Zahn, Yu. Prots, H. Borrmann and R. Kniep, *Chem. Eur. J.*, 2007, **13**, 1737.
21 W.-T. Yang, J.-Y. Li, J. Xu, H.-Z. Xing, L. Wang, J.-H. Yu and R.-R. Xu, *Solid State Sci.*, 2011, **13**, 757.
22 G. M. Sheldrick, a program for the Siemens Area Detector ABSorption correction, University of Gottingen, **1997**.
23 G. M. Sheldrick, *SHELXS-97*, Program for Crystal Structure Solution; University of Gottingen: Gottingen, Germany, **1997**; G. M. Sheldrick, *SHELXL-97*, Program for Crystal Structure Refinement; University of Gottingen: Gottingen, Germany, **1997**.
24 A. Guesmi and A. Driss, *Acta Cryst. C*, 2012, **68**, 55.
25 A. Baykal, M. Klzilyalli and R. Kniep, *J. Mater. Sci.*, 2000, **35**, 4621.
26 M. Yang, J.-H. Yu, J.-C. Di, J.-Y. Li, P. Chen, Q.-R. Fang, Y. Chen and R.-R. Xu, *Inorg. Chem.*, 2006, **45**, 3588.
27 T. Su, H.-Z. Xing, J. Xu, J.-H. Yu and R.-R. Xu, *Inorg. Chem.*, 2011, **50**, 1073.
28 M. Yang, F.-F. Xu, Q.-S. Liu, P.-F. Yan, X.-M. Liu, C. Wang and U.-W. Biermann, *Dalton Trans.*, 2010, **39**, 10571.
29 Y. X. Huang, G. Schafer, W. C. Cabrera, R. Cardoso, W. Schnelle, J. T. Zhao and R. Kniep, *Chem. Mater.*, 2001, **13**, 4348.
30 W.-T. Yang, J.-Y. Li, T.-Y. Na, J. Xu, L. Wang, J.-H. Yu and R.-R. Xu, *Dalton Trans.*, 2011, **40**, 2549.
31 G.-M. Wang, M. Valldor, C. Lorbeer and A.-V. Mudring, Eur. J. *Inorg. Chem.*, 2012, **18**, 3032.
32 Y.-Q. Feng, M. Li, H.-T. Fan, Q.-Z. Huang, D.-F. Qiu and H.-Z. Shi, *Dalton Trans.*, 2015, **44**, 894.
33 F. Sanz, C. Parada, J.-M. Rojo and C.-R. Valero, *Chem. Mater.*, 1999, **11**, 2673.
34 F. Sanz, C. Parada, J.-M. Rojo and C.-R. Valero, *Chem. Mater.*, 2001, **13**, 1334.
35 H.-Y.-P. Hong, *Mater. Res. Bull.*, 1976, **11**, 173.
36 J.-B. Goodenough, H.-Y.-P. Hong and J.-A. Kafalas, *Mater. Res. Bull.*, 1976, **11**, 203.
37 J.-M. Winand, A. Pulmont and P. Tarte, *J. Mater. Sci.*, 1990, **25**, 4008.
38 R. Collongues, A. Kahn and D. Michel, *Annu. Rev. Mater. Sci.*, 1979, **9**, 123.
39 A. Martinez-Juarez, C. Pecharroman, J. E. Iglesias and J. M. Rojo, *J. Phys. Chem. B*, 1998, **102**, 372.